JCB Article

Myo4p and She3p are required for cortical ER inheritance in *Saccharomyces cerevisiae*

Paula Estrada,[1,2] Jiwon Kim,[1,2] Jeff Coleman,[2] Lee Walker,[1,2] Brian Dunn,[2] Peter Takizawa,[2] Peter Novick,[2] and Susan Ferro-Novick[1,2]

[1]Howard Hughes Medical Institute and [2]Department of Cell Biology, Yale University School of Medicine, New Haven, CT 06519

Myo4p is a nonessential type V myosin required for the bud tip localization of *ASH1* and *IST2* mRNA. These mRNAs associate with Myo4p via the She2p and She3p proteins. She3p is an adaptor protein that links Myo4p to its cargo. She2p binds to *ASH1* and *IST2* mRNA, while She3p binds to both She2p and Myo4p. Here we show that Myo4p and She3p, but not She2p, are required for the inheritance of cortical ER in the budding yeast *Saccharomyces cerevisiae*. Consistent with this observation, we find that cortical ER inheritance is independent of mRNA transport. Cortical ER is a dynamic network that forms cytoplasmic tubular connections to the nuclear envelope. ER tubules failed to grow when actin polymerization was blocked with the drug latrunculin A (Lat-A). Additionally, a reduction in the number of cytoplasmic ER tubules was observed in Lat-A–treated and *myo4Δ* cells. Our results suggest that Myo4p and She3p facilitate the growth and orientation of ER tubules.

Introduction

During cell division, organelles are duplicated or fragmented and then partitioned into daughter cells. The accurate segregation of organelles from mother to daughter cells during the cell cycle can occur either randomly or by an ordered process that requires cellular machinery. A growing body of data suggests that the latter is the more common mechanism (Warren and Wickner, 1996; Yaffe, 1999; Catlett and Weisman, 2000). Although the inheritance of some organelles, such as the mammalian Golgi, the yeast vacuole, and mitochondria, has been investigated in some detail, less is known about the inheritance of the ER.

In the budding yeast *Saccharomyces cerevisiae* the ER has been divided into two classes: perinuclear ER and cortical or peripheral ER (Rose et al., 1989; Preuss et al., 1991). The perinuclear ER surrounds the nucleus, while the cortical ER forms a highly dynamic network of interconnected tubules that line the cell periphery. Like peripheral ER in mammalian cells, cortical ER undergoes ring closure and tubule branching movements (Prinz et al., 2000). During cell division, the first ER elements observed in the growing bud are cytoplasmic ER tubules oriented along the mother–bud axis (Du et al., 2001). These tubules either associate with the prebud site and are passively pulled into the growing bud (Fehrenbacher et al., 2002) or migrate into the daughter cell very soon after bud emergence (Du et al., 2001). The appearance of tubules aligned along the mother–bud axis suggests that a polarized structure is used for their orientation. The actin cytoskeleton is a likely candidate for this structure, as actin filaments are required for the inheritance of other organelles and for ER dynamics and motility (Catlett et al., 2000; Prinz et al., 2000; Fehrenbacher et al., 2002; Wöllert et al., 2002).

Type V myosins are actin-associated motors required for the polarized distribution of organelles, proteins, and mRNAs. These highly conserved myosins contain a number of structural elements that include an NH_2-terminal motor domain that binds to actin filaments and a COOH-terminal tail domain that binds cargo (Cheney et al., 1993; Tabb et al., 1998). In the squid giant axon, ER vesicles are transported on actin filaments by myosin V (Tabb et al., 1998). Loss of myosin Va, encoded by the mouse *dilute* locus, leads to neurological disorders that may result from defects in the transport of smooth ER from the dendritic shaft to the dendritic spine. The lightened coat color of dilute mice reflects a defect in melanosome transport (Wu et al., 1997). In plants, the actin network has been implicated in the maintenance of ER organization (Foissner et al., 1996; Boevink et al., 1998),

P. Estrada and J. Kim contributed equally to this paper.

The online version of this article includes supplemental material.

Address correspondence to Susan Ferro-Novick, Department of Cell Biology, Yale University School of Medicine, Boyer Center for Molecular Medicine, Howard Hughes Medical Institute, 295 Congress Ave., Room 254B, New Haven, CT 06519-1418. Tel.: (203) 737-5207. Fax: (203) 737-5746. email: susan.ferronovick@yale.edu

Key words: cortical ER inheritance; Myo4p; She proteins; myosin; yeast

Abbreviations used in this paper: Lat-A, latrunculin A; SC, synthetic complete.

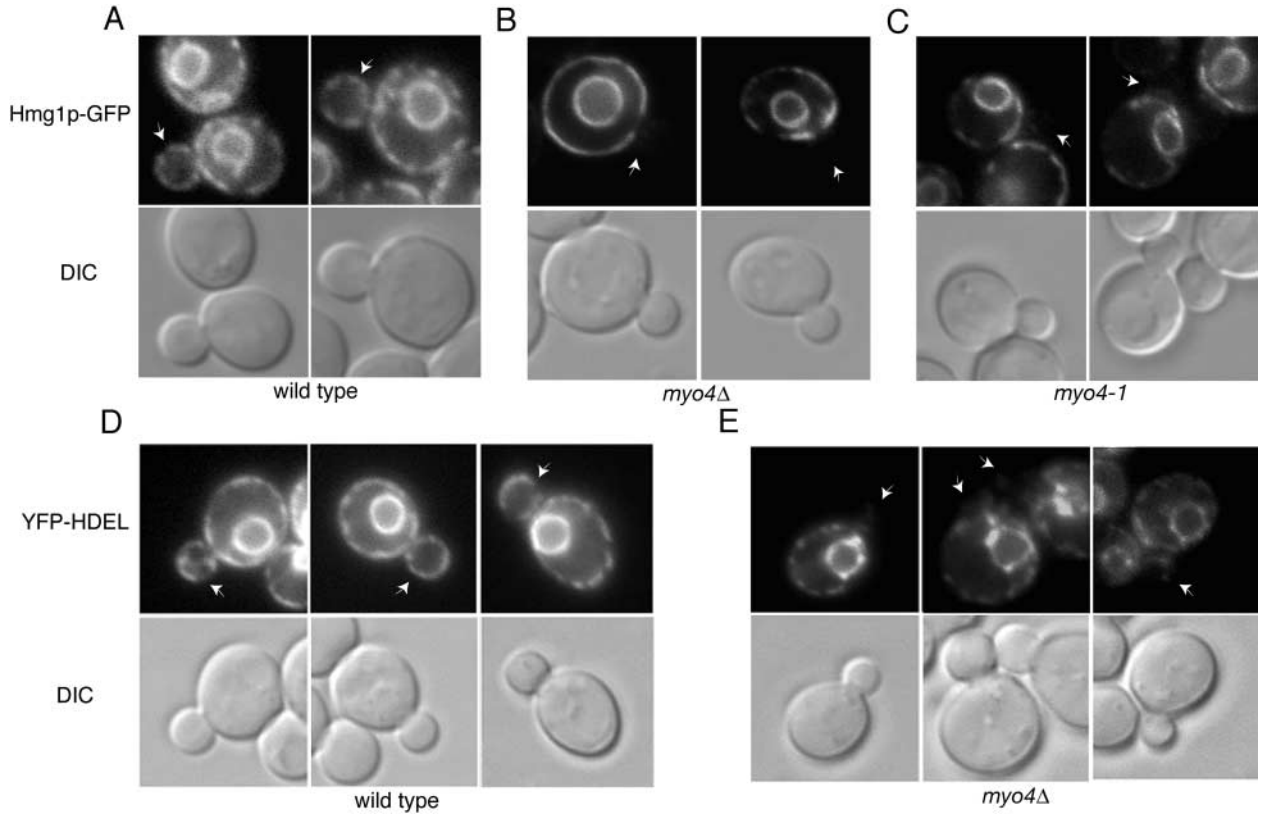

Figure 1. **Myo4p is required for the delivery of cortical ER to the periphery of daughter cells.** Wild-type and mutant cells expressing the ER markers Hmg1p-GFP (A, B, and C) or YFP-HDEL (D and E) were grown at 30°C in SC media with the appropriate amino acids. Arrows point to small buds (0.3–0.5 diameter of mother cell) in wild-type (A and D) and *myo4* mutant cells (B, C, and E). The *myo4-1* mutant contains a point mutation in the ATP-binding region of the motor domain (G171E). Cells were analyzed using fluorescence microscopy.

and in *Characea* algae, the binding and sliding of ER membranes occurs along actin filaments (Kachar and Reese, 1988).

In *S. cerevisiae*, there are two type V myosins, Myo2p and Myo4p. Myo4p is a nonessential myosin required for the asymmetric distribution of *ASH1* and *IST2* mRNAs (Long et al., 1997; Takizawa et al., 2000). *ASH1* mRNA binds to She2p, and the resulting RNA protein complex then binds to the adaptor protein She3p. She3p associates with Myo4p, and the fully assembled complex moves along actin cables to the bud tip (Bertrand et al., 1998; Böhl et al., 2000; Long et al., 2000). Ash1p then acts to inhibit mating type switching in daughter cells by repressing HO endonuclease expression (Bobola et al., 1996; Sil and Herskowitz, 1996). A similar mechanism of transport involving the She proteins is thought to regulate the asymmetric distribution of *IST2* mRNA (Takizawa and Vale, 2000). Myo2p orients the mitotic spindle during the cell cycle (Yin et al., 2000). It is also required for polarized secretion (Govindan et al., 1995; Pruyne et al., 1998), and it is essential for the delivery of late Golgi elements (Rossanese et al., 2001), the vacuole (Catlett and Weisman, 1998), and mitochondria (Itoh et al., 2002) into daughter cells. Although it is clear that the transport of these organelles into daughter cells is dependent on an actin track (Simon et al., 1997; Hill et al., 1996; Rossanese et al., 2001) and a Myo2p motor, the role of actin and myosin motors in the inheritance of ER has been elusive. Here we show that actin, Myo4p, and She3p are required for the inheritance of cortical ER.

Table I. **Quantitation of ER inheritance in wild-type and *myo4Δ* cells**

	Small buds[a]	Large buds without nuclei[b]	Large buds with nuclei[b]
	No ER in bud	**No ER in bud**	**No ER in bud**
Wild type (Hmg1p-GFP)	1/96 1%	2/17 12%	3/123 2%
myo4Δ (Hmg1p-GFP)	66/91 73%	70/92 76%	103/142 73%
Wild type (YFP-HDEL)	2/92 2%	1/32 3%	0/54 0%
myo4Δ (YFP-HDEL)	76/102 75%	49/73 67%	56/85 66%

[a]Small buds: 0.3–0.5 diameter of mother cell.
[b]Large buds: >0.5 diameter of mother cell.

Results

Myo4p is required for the inheritance of cortical ER from mother to daughter cells

To identify new genes whose products play a role in the inheritance of cortical ER, we initiated a screen of the yeast deletion library. The Hmg1p-GFP fusion protein (NH_2-terminal transmembrane domain of HMG-CoA reductase isozyme 1 fused to GFP), used as an ER marker in our studies, was described and characterized in an earlier report (Du et al., 2001). The gene encoding this fusion protein was cloned into a *CEN* (*LEU2*) plasmid and then transformed

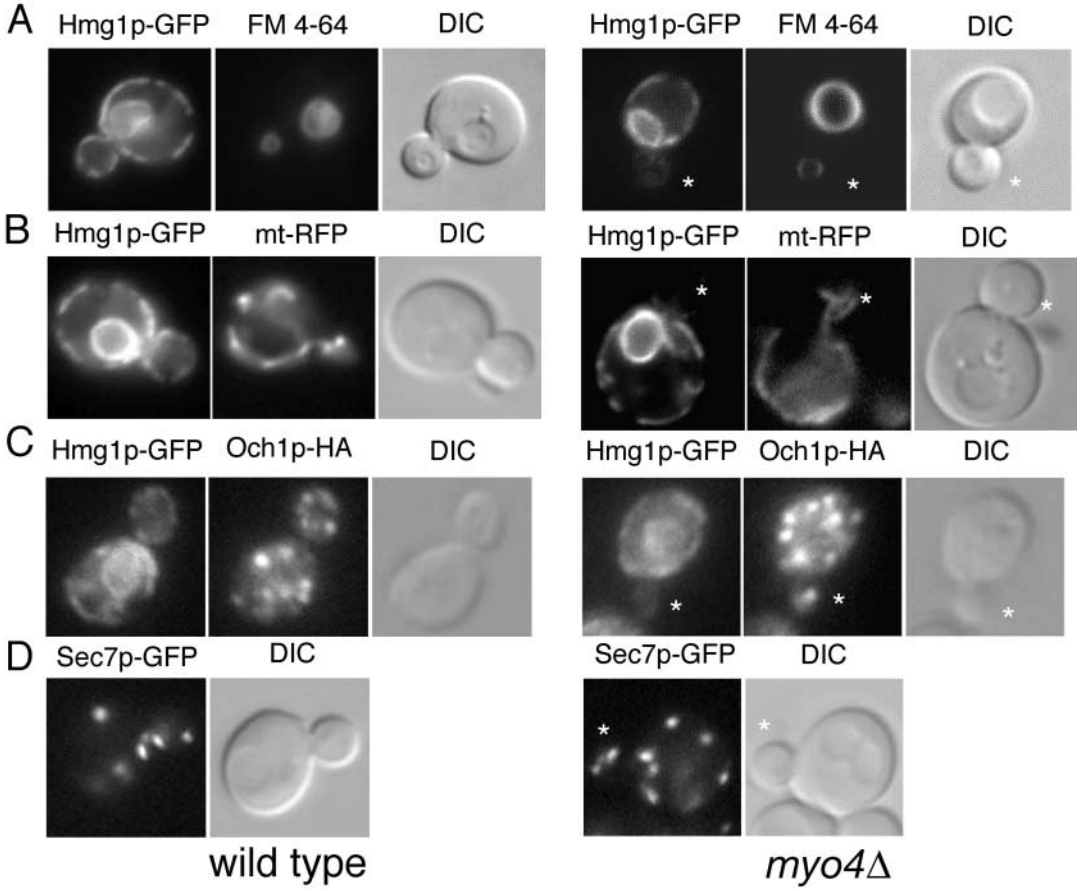

Figure 2. **The organelle inheritance defect in *myo4Δ* appears to be specific for the ER.** Organelle distribution in small buds with a volume 4–13% of the mother was analyzed by fluorescence microscopy in wild-type and *myo4Δ* mutants expressing the ER marker Hmg1p-GFP (A–C, left). The vacuole was visualized using the lipophilic dye FM 4-64 (A, middle). The mitochondria were observed in cells transformed with a plasmid expressing the F_0 ATP synthase mitochondrial targeting sequence fused to RFP (Mozdy et al., 2000) (B, middle). Using the marker Och1p-HA, the early Golgi complex was observed by indirect immunofluorescence with a monoclonal antibody directed against the HA epitope (C, middle). The late Golgi complex was examined in SFNY1240 and SFNY1280 cells expressing Sec7p-GFP (D, left). Asterisks point to the small buds of *myo4Δ* mutants.

into the deletion library with the aide of a 96-well microdispenser. After screening 768 deletion mutants, a strain containing a deletion of YAL029C was found to be defective in cortical ER inheritance. PCR analysis confirmed that this strain lacked the *myo4* gene. The remainder of this report focuses on the phenotypic characterization of cells that lack *myo4* and the role of Myo4p in ER inheritance.

To verify that the ER inheritance defect was due to the loss of *myo4* and to confirm the phenotype in our strain background, we disrupted the *myo4* gene in a wild-type strain (SFNY1054). In *myo4Δ* cells, a dramatic defect in the delivery of cortical ER tubules from mother to daughter cells was observed (Fig. 1, compare B with A). Approximately 73% of the *myo4Δ* small-budded cells (bud diameter between 0.3 and 0.5 of the mother) displayed a defect in cortical ER inheritance, while 99% of the wild-type small-budded cells acquired cortical ER (Table I). A similar percentage (76%) of mutant cells at an intermediate stage of bud growth (bud diameter >0.5 of the mother, but before nuclear segregation) also failed to contain cortical ER, while 88% of wild-type buds of the same size contained ER tubules that were uniformly distributed to the cell periphery. In cells at a late stage of bud growth (after nuclear segregation but before nuclear division), 73% of the *myo4Δ* cells displayed a defect in cortical ER inheritance (Table I). Thus, at all stages of the cell cycle leading up to nuclear division, there was a dramatic reduction in the delivery of cortical ER into the bud.

To determine if the motor activity of Myo4p plays a role in cortical ER inheritance, we constructed a point mutation in the ATP-binding region of the motor domain of Myo4p (*myo4-1)* that converted the glycine at amino acid 171 to a glutamate. As shown in Fig. 1 C, the *myo4-1* mutant displayed a defect in ER inheritance. This finding implies that the motor activity of Myo4p is required to deliver ER into daughter cells.

To confirm that the apparent defect in transport of cortical ER into daughter cells was not specific to Hmg1p-GFP, the localization of a second ER marker was examined. For these studies, a construct containing an NH_2-terminal signal sequence and a COOH-terminal ER retrieval HDEL signal, fused to YFP, was transformed into the *myo4Δ* mutant. In wild type, the localization pattern of YFP-HDEL was similar to that of Hmg1p-GFP (Fig. 1, compare D with A). Quantitation of the YFP-HDEL localization pattern revealed that >95% of buds in the different stages of growth contained cortical ER (Table I). In the *myo4Δ* mutant expressing YFP-HDEL, most of the buds exhibited defects in cortical ER in-

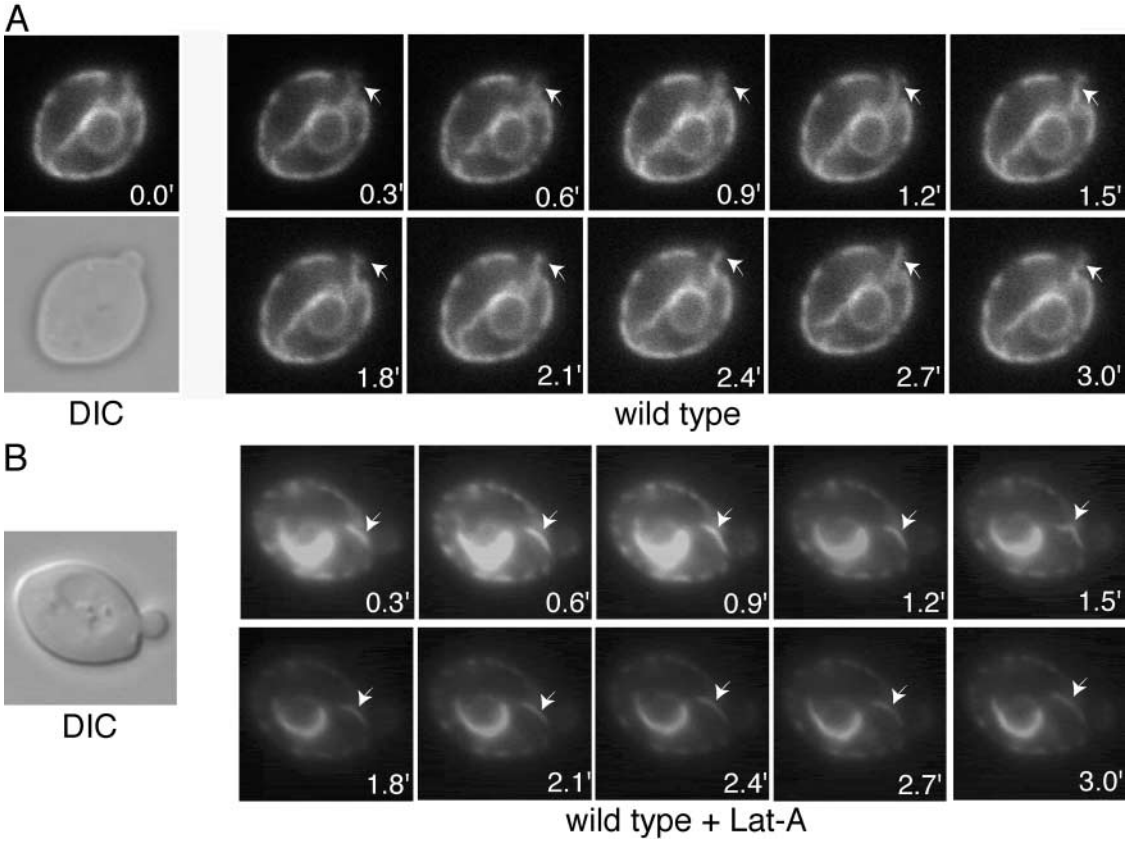

Figure 3. **ER tubules arising from the perinuclear ER of cells treated with Lat-A fail to enter the emerging bud.** Diploid wild-type cells (SFNY1061) expressing the ER marker Hmg1-GFP were grown overnight in YPD media at 30°C, treated with 200 μM Lat-A, and viewed within 10 min of treatment. The movement of tubules toward the emerging bud in the absence (A) or presence (B) of Lat-A was determined by time-lapse fluorescence microscopy at 0.3-min intervals during a 3.0-min time period. Arrows point to an ER tubule aligned along the mother–bud axis.

heritance. Approximately 75% of the small buds, 67% of the intermediate buds (before nuclear segregation), and 66% of the large buds (after nuclear segregation, but before nuclear division) failed to acquire cortical ER (Fig. 1 E and Table I). This was similar to the data obtained using Hmg1p-GFP as an ER marker protein (Table I, compare row 4 with row 2). Thus, using two different ER marker proteins, we have confirmed that cells lacking Myo4p motor activity display a dramatic, but still incomplete, defect in cortical ER inheritance.

The inheritance of other organelles is unaffected in a *myo4Δ* mutant

To determine if Myo4p is specifically required for the inheritance of cortical ER, we examined the inheritance of other organelles in the *myo4Δ* mutant. Vacuolar inheritance was examined in wild-type and *myo4Δ* cells expressing Hmg1p-GFP using the lipophilic vital dye FM4-64, which stains the vacuolar membrane (Vida and Emr, 1995). In the *myo4Δ* mutant, 137 buds that contained little to no cortical ER were examined for vacuolar inheritance. A similar number (123) of wild-type buds were also analyzed. In both wild-type and *myo4Δ* cells, all buds inherited a labeled parental vacuole (Fig. 2 A). Thus, the inheritance of vacuoles is independent of Myo4p.

The inheritance of mitochondria and Golgi elements was also examined in cells that lack Myo4p. Mitochondrial inheritance was studied by expressing a plasmid (pSFNB784), containing a mitochondrial targeting sequence fused to RFP (Mozdy et al., 2000), in wild-type and *myo4Δ* cells that contain Hmg1p-GFP. In *myo4Δ* cells, mitochondrial tubules were transported into buds that failed to inherit cortical ER (Fig. 2 B). Mitochondrial tubules were observed in 92 of the 93 *myo4Δ* buds and in 97 of the 97 wild-type buds examined. Thus, the distribution of mitochondria in wild-type and *myo4Δ* buds was essentially indistinguishable.

Sec7p is a peripheral membrane protein that is specifically localized to late Golgi membranes (Franzusoff et al., 1991; Rossanese et al., 2001). To examine the inheritance of late Golgi, the *SEC7* gene was replaced with a *SEC7-GFP* fusion in wild-type and *myo4Δ* mutant cells. The distribution of Sec7p-GFP was found to be comparable in wild type and the *myo4Δ* mutant (Fig. 2 D). In the *myo4Δ* cells, all mutant buds (122) contained late Golgi elements. The same result was observed in the 97 wild-type cells examined. Furthermore, mutant and wild-type buds contained approximately the same number of Sec7p-containing structures. These results are consistent with prior studies showing that the polarized transport of vacuoles, mitochondria, and the late Golgi requires the Myo2p motor (Hill et al., 1996; Rossanese et al., 2001; Itoh et al., 2002).

While the inheritance of the late Golgi is thought to be an actin-dependent process that requires Myo2p (Rossanese et al., 2001), less is known about the inheritance of early Golgi elements. It has been proposed that the early Golgi is de-

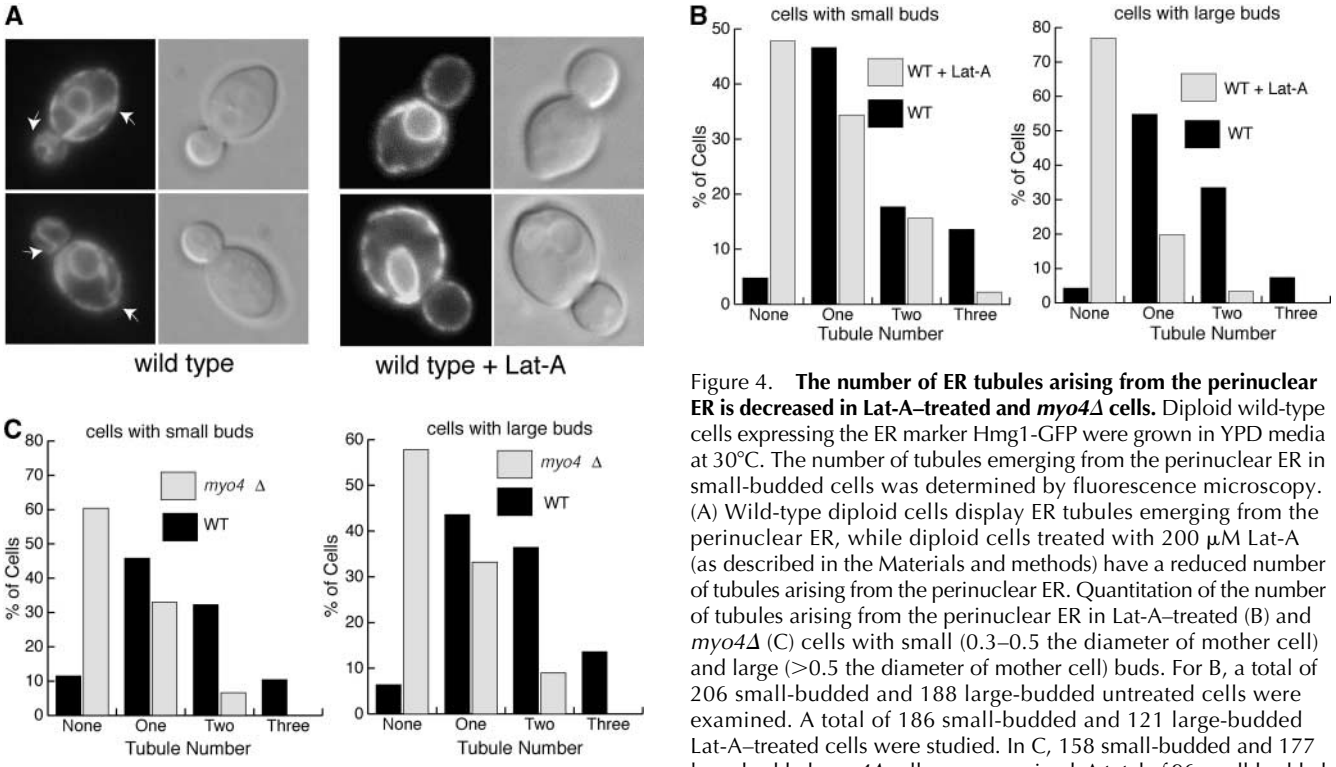

Figure 4. **The number of ER tubules arising from the perinuclear ER is decreased in Lat-A–treated and *myo4Δ* cells.** Diploid wild-type cells expressing the ER marker Hmg1-GFP were grown in YPD media at 30°C. The number of tubules emerging from the perinuclear ER in small-budded cells was determined by fluorescence microscopy. (A) Wild-type diploid cells display ER tubules emerging from the perinuclear ER, while diploid cells treated with 200 μM Lat-A (as described in the Materials and methods) have a reduced number of tubules arising from the perinuclear ER. Quantitation of the number of tubules arising from the perinuclear ER in Lat-A–treated (B) and *myo4Δ* (C) cells with small (0.3–0.5 the diameter of mother cell) and large (>0.5 the diameter of mother cell) buds. For B, a total of 206 small-budded and 188 large-budded untreated cells were examined. A total of 186 small-budded and 121 large-budded Lat-A–treated cells were studied. In C, 158 small-budded and 177 large-budded *myo4Δ* cells were examined. A total of 96 small-budded and 140 large-budded wild-type cells were studied.

rived from the ER (Rossanese et al., 1999; Bevis et al., 2002). Like the cortical ER, early Golgi membranes enter daughter cells at an early stage of bud growth (Preuss et al., 1992; Du et al., 2001; Rossanese et al., 2001). The inheritance of early Golgi membranes was examined by comparing the distribution of Och1p in *myo4Δ* and wild-type cells. Och1p is a carbohydrate-modifying enzyme that defines one of the earliest Golgi compartments in yeast (Nakayama et al., 1992). A plasmid expressing HA-tagged Och1p was transformed into wild-type and *myo4Δ* mutant cells, and the distribution of early Golgi elements was followed by indirect fluorescence using an anti-HA monoclonal antibody. The localization of early Golgi membranes in 107 *myo4Δ* mutant cells that displayed a defect in ER inheritance was indistinguishable from that of the 103 wild-type cells examined (Fig. 2 C). Thus, Myo4p is specifically required for the inheritance of cortical ER and not the inheritance of the vacuole, mitochondria, and early or late Golgi. These findings imply that the two type V myosins in yeast, Myo4p and Myo2p, have distinct and nonoverlapping functions in organelle inheritance.

Growth of ER tubules into the bud

Cytoplasmic ER tubules are readily observed in wild-type cells expressing Hmg1p-GFP. These tubules emanate from the perinuclear region, and some extend toward the bud (Fig. 3 A and Fig. 4 A). Time-lapse imaging revealed that a subset of these tubules appear to grow into the bud, suggesting that they give rise to cortical ER in the daughter cell. We found that tubule growth required polymerized actin, as cells treated with the actin-depolymerizing drug latrunculin A (Lat-A) failed to extend tubules into the bud (Fig. 3 B).

We estimated, from 10 movies of ER tubule tip movement (see Videos 1–10, available at http://www.jcb.org/cgi/content/full/jcb.200304030/DC1), that the average length of movement is 1.6 μm. The average rate is 0.013 μm/s with a standard deviation of 0.0015 μm/s. The tight clustering of the rates, as well as the vectorial nature of the extension, is consistent with a motor driven process. The rate of ER tubule tip movement is, however, substantially slower than the maximal rate observed for the Myo4p-driven movement of actin fibers in vitro (Reck-Peterson et al., 2001). These findings suggest that Myo4p may play a role in forming and extending ER tubules, and that the velocity of tubule extension is limited by tubule growth and not the motor activity of Myo4p. Interestingly, the rate of tubule extension that we have observed is similar to the elongation rate of ER tubules in animal cells (Waterman-Storer and Salmon, 1998). Because tubules are seen within the bud soon after bud emergence and are initially quite faint, we could not exclude the possibility that tubules below our limit of detection associate with the prebud site and are passively pulled into the bud as it grows, as suggested by prior studies (Fehrenbacher et al., 2002).

The number of cytoplasmic tubules are reduced in Lat-A–treated and *myo4Δ* cells

To determine if actin and Myo4p play a role in the formation or stability of cytoplasmic ER tubules, we examined cells expressing Hmg1p-GFP and quantified the number of ER tubules. We found that ~90% of wild-type cells contained at least one ER tubule, with 30–40% containing more than one tubule (Fig. 4 B). The number of tubules formed was similar in small- and large-budded cells. In contrast, treatment with Lat-A reduced the percentage of cells with at least one tubule

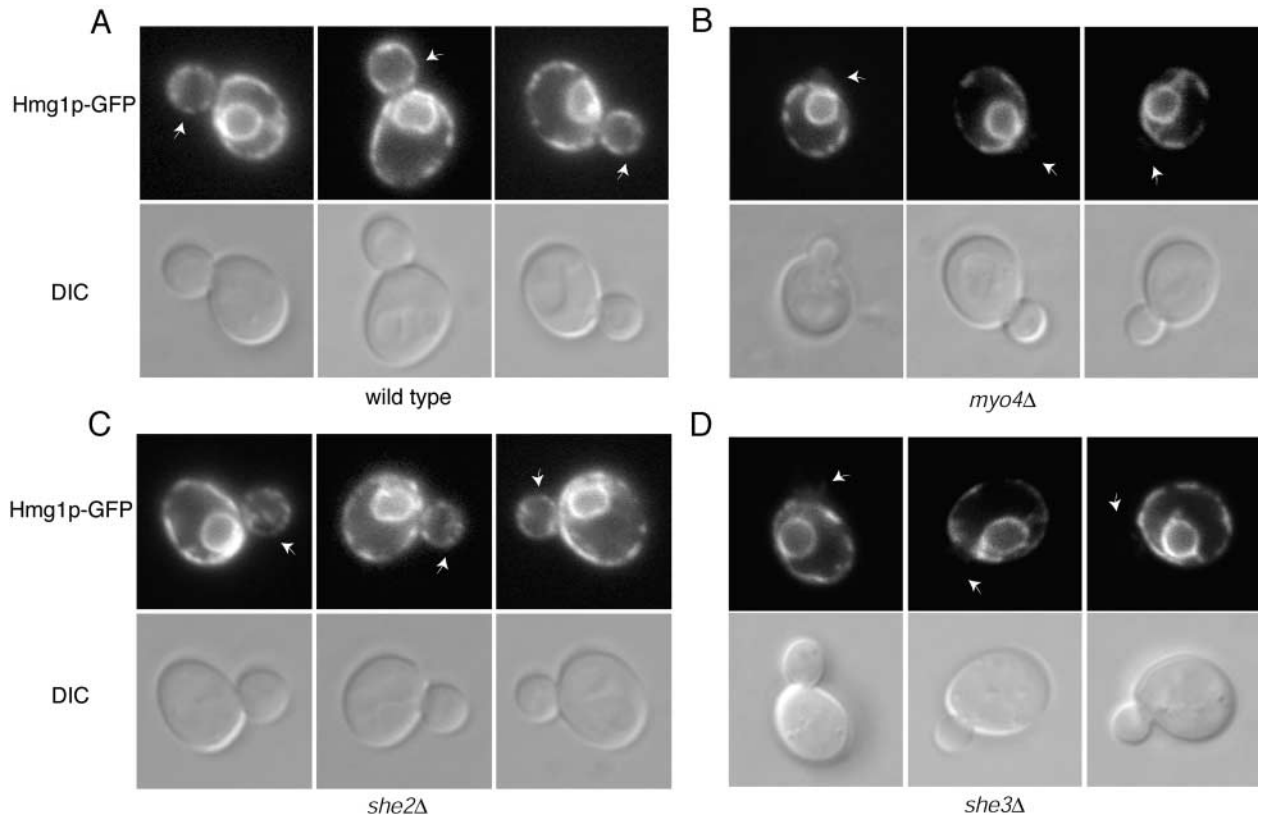

Figure 5. **She3p, but not She2p, is required for the delivery of cortical ER into the emerging bud.** Wild-type (A), *myo4Δ* (B), *she2Δ* (C), and *she3Δ* (D) mutant cells from the ResGen library, expressing the ER marker Hmg1p-GFP, were grown in SC media with the appropriate amino acids at 25°C and analyzed. PCR analysis confirmed that the correct gene was disrupted in each of the strains used in this analysis. Arrows point to small buds in wild-type and *she2Δ* cells containing cortical ER and in *myo4Δ* and *she3Δ* mutants containing no cortical ER at the cell periphery. Small buds are 0.3–0.5 diameter of the mother cell.

to ~52% of small-budded cells and ~23% of large-budded cells, demonstrating the importance of actin filaments in the formation of ER tubules (Fig. 4, A and B). In *myo4Δ* cells, the percentage of cells with at least one tubule was ~40% in both small- and large-budded cells (Fig. 4 C). Furthermore, the percentage of *myo4*Δ cells with more than one tubule was <10%. An even more dramatic result was seen when we restricted our analysis to those tubules oriented along the mother–bud axis in small-budded cells. While 90% of small-budded wild-type cells contained a cytoplasmic tubule oriented along the mother–bud axis, only 9% of small-budded *myo4Δ* cells contained such a structure (for examples see Videos 11–20, available at http://www.jcb.org/cgi/content/full/jcb.200304030/DC1). Thus, the formation, as well as orientation, of cytoplasmic ER tubules is dependent on actin and Myo4p. These findings are consistent with previous studies that implicated the actin cytoskeleton in the maintenance of ER dynamics (Prinz et al., 2000; Fehrenbacher et al., 2002).

She3p, but not She2p, is required for the inheritance of cortical ER

The binding of Myo4p to *ASH1* mRNA requires both She2p and She3p (Böhl et al., 2000; Takizawa et al., 2000). To determine if She2p and She3p play a role in the inheritance of cortical ER, we examined the delivery of Hmg1p-GFP into daughter cells in *she2Δ* and *she3Δ* strains and compared their phenotype to wild type and the *myo4Δ* mutant (Fig. 5, A and B). A dramatic delay in the delivery of cortical ER from mother to daughter cells was observed in *she3Δ* (Fig. 5 D), but not *she2Δ* (Fig. 5 C and Table II), mutant cells. In small buds with a diameter between 0.3 and 0.5 of the mother cell, ~88% of the *she3Δ* daughter cells displayed a defect in cortical ER inheritance (Table II). In wild-type buds of the same size, ~94% of the cells acquired cortical ER. In large-budded *she3Δ* cells, without nuclei, ~72% of the buds were defective for cortical ER inheritance. In larger buds in which the nucleus had not yet divided, a significant portion of the *she3Δ* buds (~38%) also showed a defect in ER inheritance (Table II). Thus, the *she3Δ* and

Table II. **Quantitation of ER inheritance in wild-type, *she2Δ*, and *she 3Δ* cells**

	Small buds[a]	Large buds without nuclei[b]	Large buds with nuclei[b]
	No ER in bud	**No ER in bud**	**No ER in bud**
Wild type	6/101 6%	0/26 0%	0/89 0%
she2Δ	13/123 11%	2/26 8%	19/104 18%
she3Δ	91/103 88%	46/64 72%	30/79 38%

[a]Small buds: 0.3–0.5 diameter of mother cell.
[b]Large buds: >0.5 diameter of mother cell.

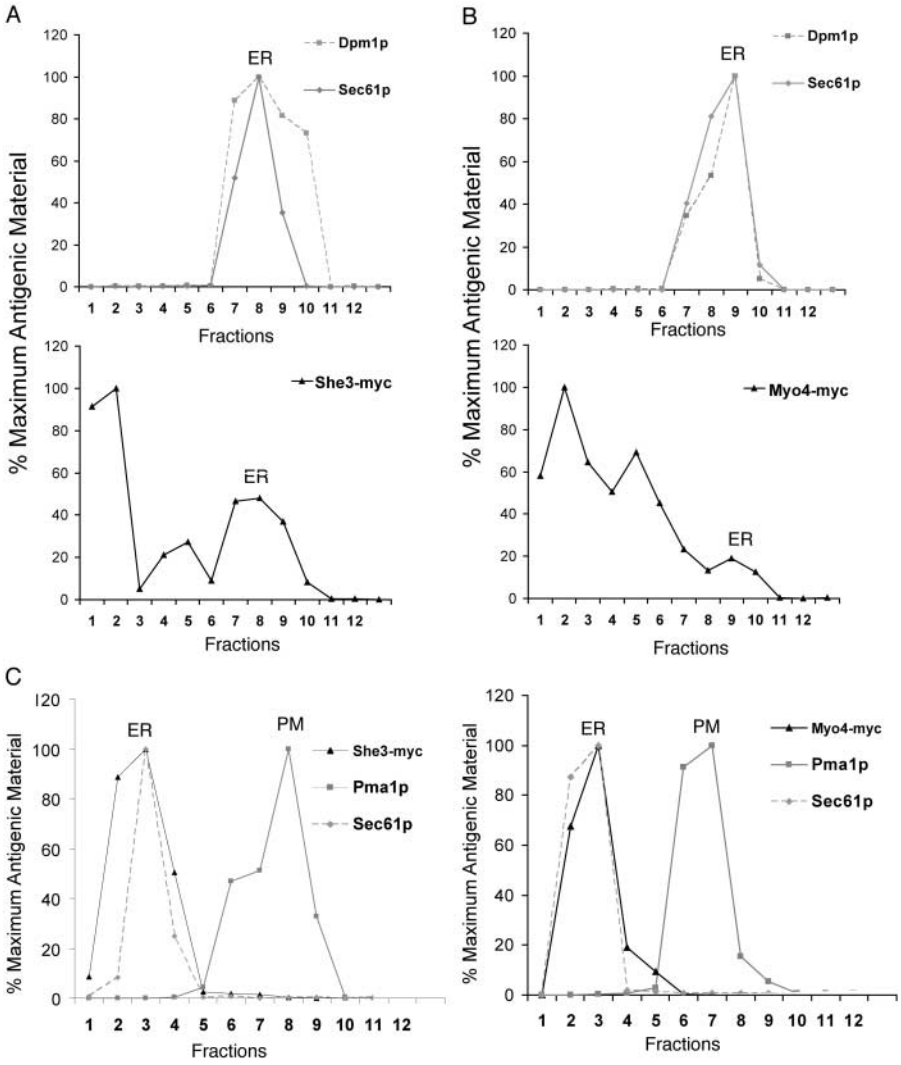

Figure 6. **She3p and Myo4p colocalize with the ER.** She3p (SFNY1264) and Myo4p (SFNY1221) were tagged with the 13x-myc epitope at the COOH terminus in cells expressing the ER marker Hmg1p-GFP. Cells were grown in minimal media with the appropriate amino acids to early log phase at 30°C. She3-13x-myc (A, bottom, ▲) and Myo4–13x-myc (B, bottom, ▲) cofractionate on a sucrose velocity gradient with the ER markers Dpm1p (A and B, top, ■) and Sec61p (A and B, top, ◆). Myc-tagged She3p (C, ▲) and Myc-tagged Myo4p (C, ▲) colocalize with Sec61p (C, ◆) but not with the plasma membrane marker Pma1p (C, ■) on an EDTA sucrose density gradient.

myo4Δ mutants have a similar phenotype. These findings indicate that She3p, but not She2p, is required for the inheritance of cortical ER. The defect in ER inheritance observed in the *myo4Δ* and *she3Δ* mutants is not a secondary consequence of disrupting the actin network, as the loss of Myo4p and She3p does not alter actin assembly (unpublished data).

Myo4p and She3p cofractionate with the ER

One prediction of the finding that Myo4p and She3p are required for ER inheritance is that both of these proteins should associate with the ER. Subcellular fractionation was performed to localize Myo4p and its adaptor protein She3p on a sucrose gradient that resolves the ER from other intracellular membranes (Antebi and Fink, 1992; Barrowman et al., 2000). Strains expressing either She3p-myc (SFNY1264) or Myo4p-myc (SFNY1221) were used to detect She3p and Myo4p. The presence of a 13myc tag on either protein did not affect ER inheritance or *ASHI* RNA localization (unpublished data; Takizawa and Vale, 2000). Lysates were prepared from SFNY1264 and SFNY1221, and the distribution of She3p and Myo4p, relative to the ER marker proteins Sec61p and Dpm1p (Wilkinson et al., 1996; Preuss et al., 1991), was determined by Western blot analysis. In several gradients, a substantial amount of the She3p (26–46%) cofractionated with the ER (Fig. 6 A), while a smaller portion (~5–10%) of the Myo4p was found in ER fractions (Fig. 6 B). The amount of She3p and Myo4p associated with the ER may vary, as peripheral membrane proteins tend to shear off membranes during lysis. The localization of She3p and Myo4p was unchanged when lysates prepared from *she2Δ* strains expressing either She3p-myc or Myo4p-myc were fractionated (Fig. 7, A and B). The same results were also obtained when lysates expressing She3p-myc (Fig. 7 C) or Myo4p-myc (not depicted) were treated with RNase. Thus, the interaction of the Myo4p–She3p motor complex with the ER is not mediated by an associated RNA.

As the ER cofractionates with the plasma membrane on this gradient, we stripped the ER of ribosomes by fractionating extracts on a sucrose density gradient in the presence of EDTA, as described before (Roberg et al., 1997). As shown in Fig. 6 C, the ER fractionated at the top of the gradient and was well resolved from the more dense plasma membrane. Furthermore, She3p cofractionated with the ER and not the plasma membrane. The same result was obtained when Myo4p was localized on this gradient (Fig. 6 C). As the adaptor protein She3p and the class V myosin Myo4p form a complex (Takizawa and Vale, 2000) and both proteins cofractionate with the ER, these findings imply that the Myo4p–She3p motor complex is directly associated with the ER.

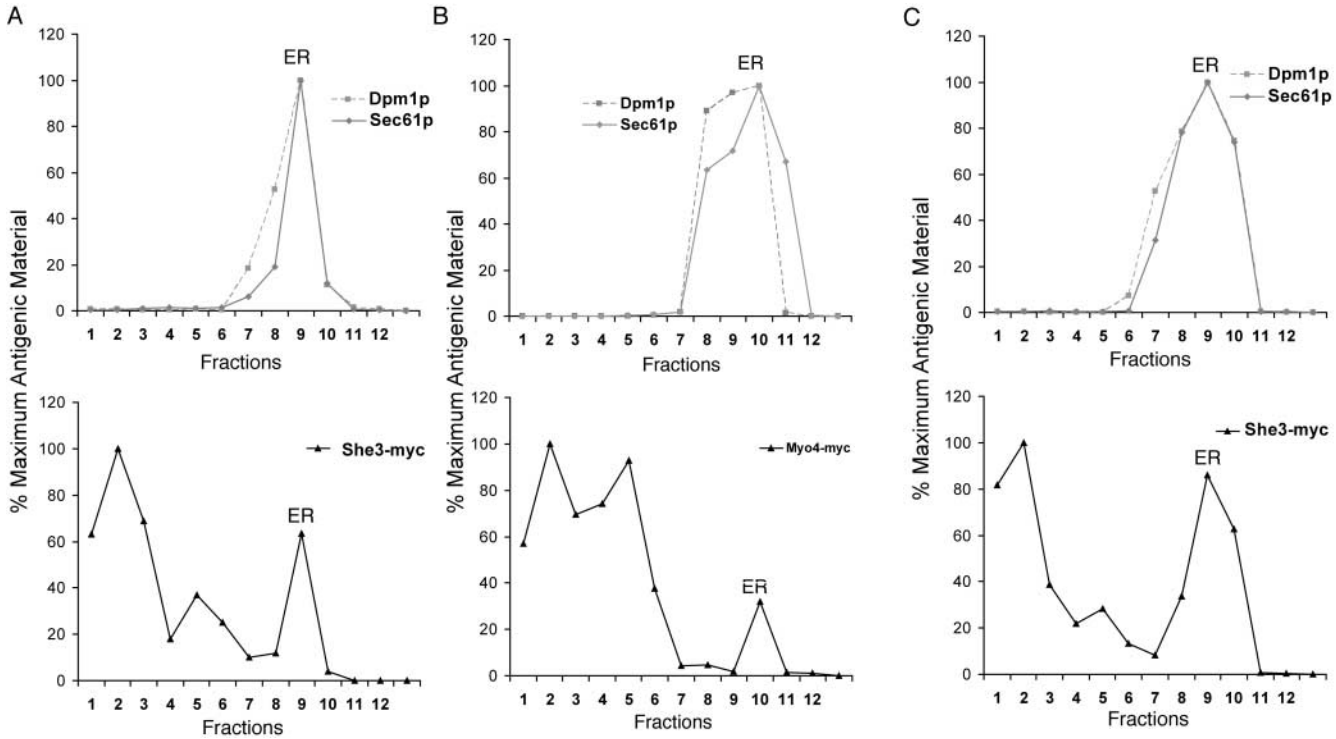

Figure 7. **She3p and Myo4p colocalize with the ER in the absence of She2p.** She3p (SFNY1265) and Myo4p (SFNY1266) were tagged with the 13x-myc epitope at the COOH terminus in *she2Δ* cells expressing the ER marker Hmg1p-GFP. Cells were grown at 30°C in minimal media with the appropriate amino acids to early log phase. (A) She3p-13x-myc (bottom, ▲) and (B) Myo4–13x-myc (bottom, ▲) cofractionate on a sucrose velocity gradient with the ER markers Dpm1p (A and B, top, ■) and Sec61p (A and B, top, ◆). (C) A lysate prepared from myc-tagged She3p (SFNY 1264) was treated with RNase A for 5 min and then fractionated on a sucrose velocity gradient. Myc-tagged She3p (C, bottom, ▲) colocalizes with the ER markers Sec61p (C, top, ◆) and Dpm1p (C, top, ■).

Cortical ER inheritance is not required for the asymmetric distribution of mRNA

The finding that the Myo4p–She3p complex is required for ER inheritance raises the possibility that the asymmetric distribution of mRNA is dependent on cortical ER inheritance. To address this question, the localization of *IST2* mRNA (Takizawa et al., 2000), which localizes to the bud tip throughout the cell cycle, was examined in the *aux1* mutant, which is defective in ER inheritance (Du et al., 2001). *AUX1* encodes a hydrophilic protein of 668 amino acids. The COOH terminus of Aux1p contains a J-domain that is homologous to the J-domain of the clathrin uncoating protein auxilin (Holstein et al., 1996). Aux1p may be a bifunctional protein, as the loss of the J-domain leads to vacuole fragmentation and membrane accumulation but does not affect the segregation of ER into daughter cells (Du et al., 2001). We found that *IST2* mRNA localized to the bud tip in wild-type cells and in an *aux1Δ* mutant, lacking the entire *AUX1* gene (Fig. 8 A). Similar results were obtained when the localization of *ASH1* mRNA was examined (not depicted). Thus, cortical ER inheritance is not required for the localization of mRNA to the bud tip.

To determine if cortical ER inheritance and mRNA transport are independent processes, we constructed a mutant in *she3* that disrupts the She2p binding site. Previous studies (Böhl et al., 2000) have shown that She3p binds to She2p via the COOH terminus of She3p (amino acids 213–426). To disrupt the interaction of She3p with She2p, we deleted the last 176 amino acids of She3p (see diagram in Fig. 8 B). As anticipated, *IST2* mRNA failed to localize to the bud tip in this mutant (Fig. 8 C). In contrast, truncation of the COOH terminus of She3p had no effect on ER inheritance (Fig. 8 C). These findings demonstrate that different domains of She3p are required for mRNA localization and ER inheritance.

Discussion

There are two type V myosins in yeast, Myo2p and Myo4p. Myo2p binds to a variety of cargo. It has been implicated in the polarized delivery of secretory vesicles (Govindan et al., 1995; Pruyne et al., 1998) and in the inheritance of several organelles (Catlett and Weisman, 1998; Rossanese et al., 2001; Itoh et al., 2002). Myo2p also plays a role in orienting the spindle during the cell cycle (Yin et al., 2000). However, until this study, the only known role for Myo4p was in the localization of *ASH1* and *IST2* mRNAs to the bud tip.

Proper localization of *ASH1* and *IST2* mRNA requires the *SHE* genes (Bobola et al., 1996; Jansen et al., 1996; Takizawa et al., 2000). *ASH1* and *IST2* bind to She2p, while She3p links Myo4p to the She2p–mRNA complex (Böhl et al., 2000; Takizawa and Vale, 2000). Movement of the She2p–mRNA ribonucleoprotein complex along actin cables is myosin dependent, and the deletion of *myo4*, *she2*, or *she3* prevents these mRNAs from localizing to the bud tip (Jansen et al., 1996; Long et al., 1997).

Cortical ER enters daughter cells in a polarized fashion. It is enriched at the presumptive bud site and accumulates at the

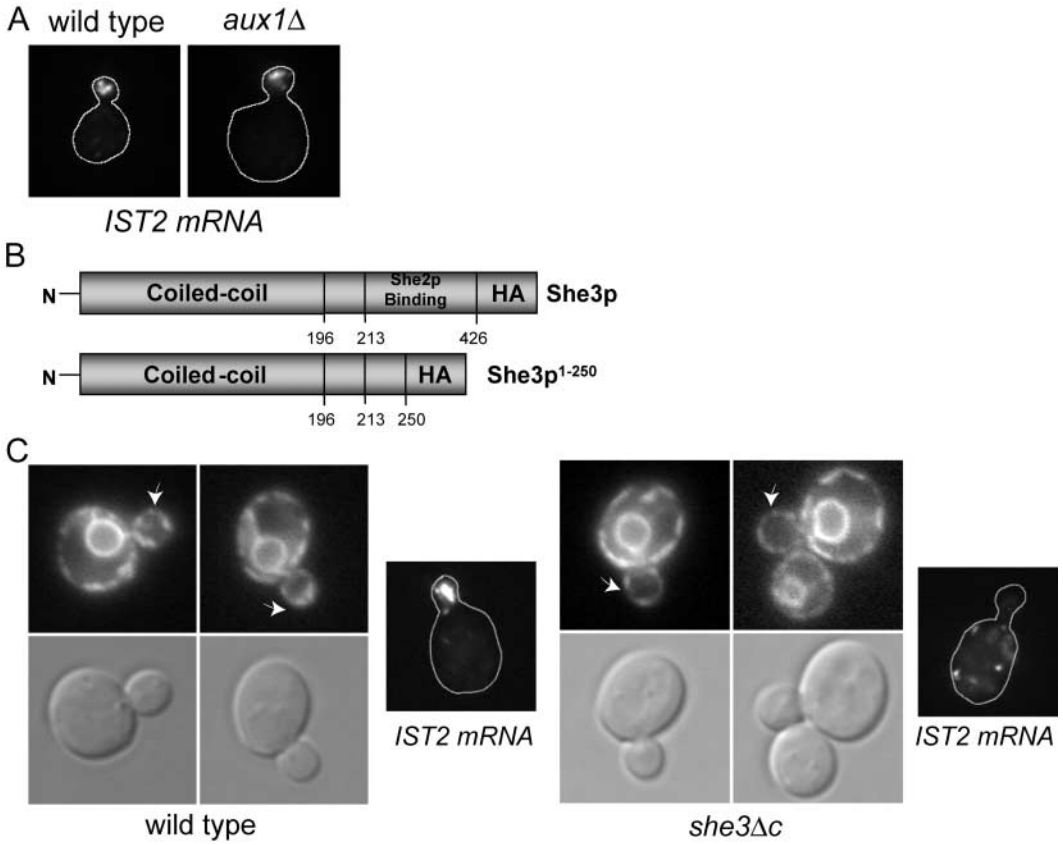

Figure 8. **Inheritance of cortical ER does not require the asymmetric distribution of mRNA.** (A) Localization of *IST2* mRNA. *IST2* mRNA distribution was determined in wild-type and *aux1Δ* small-budded cells by in situ hybridization (Takizawa et al., 2000). *IST2* mRNA was observed at the bud tip in both wild type and the mutant. Note that *aux1* mutant cells are slightly larger than wild type. (B) Schematic of She3p constructs used to study cortical ER inheritance. The top construct represents full-length She3p expressed in SFNY1303, and the bottom construct depicts a She3p truncation lacking 176 amino acids from its COOH terminus expressed in SFNY1310. The numbers correspond to the amino acid position. (C) Inheritance of cortical ER does not require the She2p-binding domain of She3p. SFNY1303 (wild type) and SFNY 1310 (*she3Δc*) cells expressing the ER marker Hmg1p-GFP were grown at 30°C in SC media with the appropriate amino acids. Arrows point to the cortical ER at the periphery of small buds. *IST2* mRNA is mislocalized in *she3Δc* cells. mRNA distribution was analyzed as described in A.

bud tip in small- and medium-sized buds (Fehrenbacher et al., 2002). Myo4p, which is required for this process, localizes to the cortex and bud tip (Jansen et al., 1996; Münchow et al., 1999) and is enriched in the bud by a retention mechanism that involves the RNA binding protein She2p (Kruse et al., 2002). Here we have identified a role for Myo4p in cortical ER inheritance. We show that the role of Myo4p in organelle inheritance is distinct from that of Myo2p. While Myo4p is required for ER inheritance, it is not required for the inheritance of vacuoles, mitochondria, and late Golgi elements, events known to be dependent on Myo2p (Hill et al., 1996; Rossanese et al., 2001; Itoh et al., 2002). Our findings indicate that the deletion of *myo4* and *she3*, but not *she2*, results in a partial block in the delivery of cortical ER from mother to daughter cells. Furthermore, deletion of *myo4* or inhibition of actin polymerization with the drug Lat-A leads to a significant reduction in the number of ER tubules in the cytoplasm. Tubules oriented along the mother–bud axis in small-budded cells are most dramatically affected. Cytoplasmic ER tubules also fail to enter daughter cells subsequent to Lat-A treatment. Myo4p and She3p may be needed for the growth and orientation of cytoplasmic ER tubules into daughter cells.

Although the deletion of either *myo4* or *she3* leads to a dramatic loss of cortical ER in daughter cells, ~25% of the buds still receive ER elements. Treatment of *myo4Δ* cells with nocodazole did not decrease the amount of cortical ER found in the bud (unpublished data), indicating that the ER that enters the bud in *myo4Δ* cells is not microtubule dependent. These findings indicate that a Myo4p/She3p-independent mechanism can function to transmit ER into daughter cells, albeit inefficiently. Additional studies will be needed to define the nature of this secondary pathway to ER inheritance.

In neurons, the ER is transported on actin by myosin V (Tabb et al., 1998), and myosin V drives ER network formation in *Xenopus* egg extracts (Wöllert et al., 2002). Thus the growth, formation, and movement of ER by myosin V along actin is a highly conserved process. Our finding that both Myo4p and She3p physically associate with ER membranes implies that both of these proteins play a direct role in the inheritance of ER. Interestingly, a larger fraction of the She3p cofractionated with the ER. This suggests that She3p may link Myo4p to ER tubules. The finding that *she3Δ* cells display a defect in ER inheritance is consistent with this proposal. Although the interaction between Myo4p and *ASH1* mRNA is dependent on She2p (Münchow et al., 1999), the association of She3p and Myo4p with ER membranes is not. Consistent with this result, we find that the loss of She2p does not lead to a defect in cortical ER inheritance, and that

Table III. **Strains used in this study**

Strain	Genotype	Source
NY873	*MAT**a** his3-Δ200 lys2-801 leu2-3, 112 ura3-52*	Novick collection
NY1211	*MATα Gal*$^+$ *his3-Δ200 leu2-3, 112 ura3-52*	Novick collection
SFNY1054	*MAT**a** his3-Δ200 lys2-801 leu2-3, 112 ura3-52*::(*URA3 HMG1-GFP*)	Ferro-Novick collection
SFNY1061	*MAT**a**/α his3-Δ200/his3-Δ200 lys2-801/lys2-801 leu2-3, 112/leu2-3, 112 ura3-52*::(*URA3 HMG1-GFP*)/*ura3-52*::(*URA3 HMG1-GFP*)	Ferro-Novick collection
SFNY1196	*MATα Gal*$^+$ *his3-Δ200 leu2-3, 112 ura3-52* pSFNB1030 (*YFP-HDEL URA3 CEN*)	This study
SFNY1218	*MAT**a** lys2-801 leu2-3, 112 ura3-52*::(*URA3 HMG1-GFP*) *his3-Δ200 myo4Δ*::*his5*$^+$	This study
SFNY1220	*MAT**a** lys2-801 leu2-3, 112* pPT201(*myo4-1 LEU2 CEN*) *ura3-52*::(*URA3 HMG1-GFP*) *his3-Δ200 myo4Δ*::*his5*$^+$	
SFNY1221	*MAT**a** his3-11 leu2-3, 112 ura3-1 trp1-1 ade2-1 can1-100*::(*KANr MYO4-13x-myc*)	P. Takizawa collection
SFNY1224	*MAT**a** Gal*$^+$ *lys2-801 leu2-3, 112 ura3-52*::(*URA3 HMG1-GFP*) *his3-Δ200 myo4Δ*::*his5*$^+$ pSFNB784 (*PPrFoATP-dsRFP LEU2*)	This study
SFNY1225	*MAT**a** Gal*$^+$ *lys2-801 leu2-3, 112 ura3-52*::(*URA3 HMG1-GFP*) *his3-Δ200 myo4Δ*::*his5*$^+$ pSFNB637 (*pOch1p-HA LEU2*)	This study
SFNY1226	*MAT**a** lys2-801 leu2-3, 112 ura3-52*::(*URA3 HMG1-GFP*) *his3-Δ200 she2Δ*::*his5*$^+$	This study
SFNY1227	*MAT**a** lys2-801 leu2-3, 112 ura3-52*::(*URA3 HMG1-GFP*) *his3-Δ200 she3Δ*::*his5*$^+$	This study
SFNY1230	*MAT**a** his3-11 leu2-3, 112 ura3-1 trp1-1 ade2-1 can1-100*	P. Takizawa collection
SFNY1235	*MATα Gal*$^+$ *leu2-3, 112 ura3-52 his3-Δ200 myo4Δ*::*his5*$^+$	This study
SFNY1240	*MATα Gal*$^+$ *leu2-3, 112 ura3-52*::(*URA3 SEC7-GFP*) *his3-Δ200 myo4Δ*::*his5*$^+$	This study
SFNY1261	*MAT**a** his3Δ1 ura3Δ0 met15Δ0 leu2Δ0* pSFNB1000 (*HMG1-GFP LEU2 CEN*)	This study
SFNY1262	*MAT**a** his3Δ1 ura3Δ0 met15Δ0 she2Δ*::*KANr leu2Δ0* pSFNB1000 (*HMG1-GFP LEU2 CEN*)	This study
SFNY1263	*MAT**a** his3Δ1 ura3Δ0 met15Δ0 myo4Δ*::*KANr leu2Δ0* pSFNB1000 (*HMG1-GFP LEU2 CEN*)	This study
SFNY1264	*MAT**a** his3-11 leu2-3, 112 ura3-1 trp1-1 ade2-1 can1-100*::(*KANr SHE3-13x-myc*)	P. Takizawa collection
SFNY1265	*MAT**a** his3-11 leu2-3, 112 trp1-1 ade2-1 can1-100*::(*KANr SHE3-13x-myc*) *ura3-1she2Δ*::*URA3*	P. Takizawa collection
SFNY1266	*MAT**a** his3-11, leu2-3, 112 trp1-1 ade2-1 can1-100*::(*KANr MYO4-13x-myc*) *ura3-1she2Δ*::*URA3*	P. Takizawa collection
SFNY1267	*MAT**a** his3Δ1 ura3Δ0 met15Δ0 she3Δ*::*KANr leu2Δ0* pSFNB1000 (*HMG1-GFP LEU2 CEN*)	This study
SFNY1270	*MATα Gal*$^+$ *leu2-3, 112 his3-Δ200 myo4Δ*::*his5*$^+$ *ura3-52* pSFNB1030 (*YFP-HDEL URA3 CEN*)	This study
SFNY1280	*MAT**a** his3-Δ200 lys2-801 leu2-3, 112 ura3-52*::(*URA3 SEC7-GFP*)	This study
SFNY1303	*MAT**a** his3Δ1 met15Δ0 she3Δ*::*KANr leu2Δ0* pSFNB1000 (*HMG1-GFP LEU2 CEN*) *ura3Δ0* pRS316 (*SHE3 URA3 CEN*)	This study
SFNY1310	*MAT**a** his3Δ1 met15Δ0 she3Δ*::*KANr leu2Δ0* pSFNB1000 (*HMG1-GFP LEU2 CEN*) *ura3Δ0* pRS316 (*SHE3Δc URA3 CEN*)	This study

cortical ER inheritance is independent of mRNA localization. Thus, the Myo4p–She3p complex must bind to the ER via a factor other than She2p. We are currently screening the yeast deletion library to identify this unknown factor as well as additional components of the ER inheritance machinery.

Materials and methods

Plasmids and strains

Plasmid SFNB1030 (*CEN URA3*) encodes the *HDEL* signal sequence from *KAR2* fused to the COOH terminus of *YFP*. To generate this plasmid, a 0.864-kb fragment that encodes HDEL-YFP was amplified from pDN300 (a gift from David Ng, Pennsylvania State University, University Park, PA) with primers to introduce *SalI* and *SpeI* restriction sites. This PCR product was then cloned into pTEF416 (*CEN URA3*) between the *SalI* and *SpeI* sites.

SFNY1196 and SFNY1270 (Table III) were constructed by transforming NY1211 and SFNY1235, respectively, with plasmid SFNB1030 (Table III) and selecting for Leu$^+$ transformants. Strains SFNY1224 and SFNY1225 (Table III) were constructed by transforming SFNY1235 with plasmids SFNB784 and SFNB637 (Table III), respectively, and selecting for Leu$^+$ transformants.

SFNY1261, SFNY1262, SFNY1263, and SFNY1267 (Table III) were constructed by transforming BY4741, YKL130C, YAL029C, and YBR130C from the ResGen deletion library, respectively, with plasmid SFNB1000 and selecting for Leu$^+$ transformants. All deletions were confirmed by PCR analysis.

Full-length *SHE3*, in vector pRS316, was introduced into SFNY1267 to generate SFNY1303 (Table III). A *she3* truncation mutant (lacking 176 amino acids from the COOH terminus), in vector pRS316, was introduced into SFNY1267 to generate SFNY1310 (Table III), and Ura$^+$ transformants were selected. Plasmid PT201 (*CEN LEU2*), carrying a point mutation in the ATP-binding region of the motor domain of Myo4p (G171E), was transformed into SFNY1218 (Table III) to generate SFNY1220. The *myo4-1* mutant allele was obtained from Susan Brown when she was at the University of Michigan (Ann Arbor, MI).

To construct SFNY1305 (Table III), YIplac204/DsRed.T1-HDEL (a gift from Ben Glick, University of Chicago, Chicago, IL) was linearized with EcoRV and transformed into PT68, and Trp$^+$ transformants were selected.

Isolation of the *myo4* mutant

The yeast *MATa* haploid deletion library from Research Genetics (ResGen-Invitrogen Corporation) was screened to identify genes that display a defect in the inheritance of cortical ER. The library contains 4,848 ORFs that were disrupted with the KanMX module in the parent strain BY4741. Cells were transformed with plasmid SFNB1000 (*CEN*, *LEU*) using a Hydra 96 microdispenser (Robbins Scientific Corporation). Stationery cultures were generated in a 96-well assay block (Corning Inc.) by inoculating YPD (580 μl per well) with cells (10 μl) from a ResGen master plate. Glass beads (3.5 mm; Fisher Scientific) were placed in each well to facilitate airation of the cultures. The block was incubated for 3 d at 25°C.

Stationery cultures were diluted (1:1,000) in YPD and grown overnight at 25°C to an OD_{600} of 1.0–1.5. The cells were transferred (390 μl per well) to a new assay block without beads and centrifuged at 2,000 rpm for 5 min. Pellets were washed with sterile water (580 μl per well), centrifuged, resuspended in LTE (100 mM LiOAc, 10 mM Tris pH to 8.0, 1 mM EDTA; 580 μl per well), and then incubated at room temperature for 1 h. The robot was sterilized after each step in the transformation protocol by washing the teflon needles and glass wells three times in 70% ethanol followed by three washes in sterile water. The cells were then centrifuged and the pellets were resuspended in 35% PEG/LTE (405 μl per well). Transformation was performed by adding 15 μl of a 2 mg/ml stock of carrier DNA (salmon testes from Sigma-Aldrich) and 15 μl of DNA (50 ng/μl stock) from plasmid SFNB1000 (*HMG1-GFP CEN LEU2*) into each well followed by a 1-h incubation at 30°C. The cells were heat shocked for 10 min in a 42°C water bath and centrifuged. The pellets were washed in sterile water (580 μl per well), centrifuged, resuspended in synthetic complete (SC) minus Leu media (580

μl per well), and transferred to an assay block containing beads. Transformed cells were grown for 3 d at 25°C and then replica plated onto a synthetic dropout minus Leu (QBiogen) agar plate and grown for 3 d to confirm transformation. Stationary cultures were grown from colonies on the agar plate as described above. The stationery cultures were then diluted and grown overnight at 25°C in SC minus Leu to an OD_{600} of ~0.3–0.5. A total of 768 deletion strains out of the 4,848 in the library (16%) were screened.

Strain construction

SFNY1218 and SFNY1235 were generated using a PCR-based gene deletion method (Longtine et al., 1998). The forward primer, MYO4-F1 (5′-AACACAAAAAAACAAAAAAAATCCTATAACCAGTTCTCCCGCGGTCGACGGATCCCCGGGTT-3′) contained 40 nucleotides of *MYO4* gene-specific sequence located upstream of the start codon followed by 20 nucleotides of gene-specific sequence from plasmid pFA6a-His3MX6, which contains the *his5*$^+$ gene from *Schizosaccharomyces pombe* (Longtine et al., 1998). The reverse primer, MYO4-R1 (5′-TATATACATATATACATATATGGGCGTATATTTACTTTGTTCGAATTCGAGCTCGTTTAAAC-3′) contained 40 nucleotides of *MYO4* gene-specific sequence located downstream of the stop codon followed by 20 nucleotides of gene-specific sequence from plasmid pFA6a-His3MX6. The fragment was amplified, and the PCR product was transformed into SFNY1054 and NY1211 (Table III). His$^+$ transformants were selected, and replacement of the *MYO4* gene with *his5*$^+$ was confirmed by PCR. SFNY1226 and SFNY1227 (Table III) were generated by the same method with the following primers. To disrupt *SHE2*, SHE2-F1 (5′-CCCTCCTTAATTTTCCTTTTGCATAATACCAGACACTTAAAAGGTCGACGGATCCCCGGGTT-3′) was used as a forward primer and SHE2-R1 (5′-AGTGGTACTTATTTGCTCTTTTTGAGCTAAAAACTGAAGGCCGAATTCGAGCTCGTTTAAAC-3′) as a reverse primer. To disrupt *SHE3*, we used SHE3-F1 as a forward primer (5′-TATCAAGCACGCCAAGGTTCAACGACACTACTTTTGTGTAAGGGTCGACGGATCCCCGGGTT-3′) and SHE3-R1 as a reverse primer (5′-CTAAATGAATCCTATATATATACTCCCTTGTGTCGGCATATTGAATTCGAGCTCGTTTAAAC-3′).

Fluorescence microscopy

To visualize the ER or mitochondria, cells expressing DsRed, GFP, YFP, or RFP fusion proteins were grown overnight in minimal or SC media at 30°C to an OD_{600} of 0.3, pelleted, and resuspended in 30 μl of growth medium. Then 3 μl of the cell suspension was mixed with an equal volume of growth medium containing 0.6% NuSieve GTG low melting temperature agarose (FMC BioProducts).

Indirect immunofluorescence was performed according to Du et al. (2001) with the following modifications. To remove the cell wall, cells were incubated for 9 min at 30°C with gentle shaking in 1 ml of 100 mM sodium phosphate/1.2 M sorbitol buffer (pH 6.6) containing 143 mM β-mercaptoethanol and 50 μg/ml Zymolyase 100T (Seikagaku America). Spheroplasts were then washed three times with 5 ml of 100 mM sodium phosphate/1.2 M sorbitol buffer (pH 6.6) and resuspended in 250 μl of the same buffer. Subsequently, 30 μl of cells were attached to eight-well slides coated with poly-L-lysine and permeabilized in 30 μl of P buffer (1× PBS containing 0.1% SDS and 10 mg/ml BSA) for 5 min.

To visualize vacuoles in wild-type and *myo4Δ* mutant cells, vacuole membranes were labeled with 80 μM FM 4-64 (Molecular Probes) according to methods previously described (Wang et al., 1996; Du et al., 2001).

Cells were observed with a Carl Zeiss MicroImaging, Inc. Axiophot fluorescence microscope using a 100× oil-immersion objective. Images were captured with an Orca ER digital camera (model no. C4742–95; Hamamatsu Photonics) and the OpenLab 3.08 imaging software (OpenLab Inc.). Images were further processed with Adobe Photoshop 7.0 and Illustrator 10.0.

Lat-A treatment

SFNY1061 (Table III) was grown in 5 ml of YPD overnight at 30°C to an OD_{600} of 0.15. Cells were harvested and resuspended in 200 μl of YPD, and 25 μl was subsequently mounted in an equal volume of medium containing 0.6% low melting temperature agarose and 200 μM Lat-A (Molecular Probes). Cells were observed with a Carl Zeiss MicroImaging, Inc. fluorescence microscope immediately after Lat-A treatment.

Time-lapse imaging

Time-lapse fluorescence microscopy of SFNY1061 was performed on cells grown at 30°C in YPD to an OD_{600} of 0.15. Cells (untreated or treated with 200 μM Lat-A) were mounted in 0.4% agarose and viewed with a Carl Zeiss MicroImaging, Inc. fluorescence microscope. Images were captured using OpenLab software at 18-s intervals for 3 min and exported as a Quicktime file. Image stills were generated using Adobe Photoshop 7.0 and Illustrator 10.0.

Rate of tubule movement

The distance traveled was determined by measuring the tubule movement from the bud neck to the bud tip in time-lapse image stills. The ruler tool in the measurement module of OpenLab 3.1.3 was positioned on the tubule at the bud neck and was extended over the length of the tubule as it extended toward the bud tip. The distance traveled by the tubule was then recorded in micrometers. To determine the rate of movement, the distance traveled was divided by the time a tubule approached the bud tip. The time was recorded and displayed in each image still. Rate measurements are reported as micrometers per second.

Subcellular fractionation

Cells were grown, converted to spheroplasts, and lysed in the absence or presence of 100 μg/ml RNase A as described previously (Barrowman et al., 2000). 66 OD_{600} units were then fractionated on sucrose velocity gradients according to Barrowman et al. (2000). Fractions (~1 ml each) were collected from the top of the gradient, and the protein in each fraction was precipitated by adding 500 μl of cold 50% trichloroacetic acid. The protein pellets were collected by centrifugation at 14,000 rpm for 5 min at 4°C, resuspended in 66 μl of 1 M Tris, and solubilized in 99 μl of SDS sample buffer. The fractions (30 μl each) were then resolved by SDS-PAGE and subjected to Western blot analysis. The antibodies were subsequently detected by ECL (Amersham Biosciences), and the bands were quantitated using BioImage software. The data are plotted as a percent of the maximum antigenic material.

The ER and plasma membrane were fractionated on a linear sucrose density gradient in the presence of EDTA as described previously (Roberg et al., 1997). In brief, cells were grown to an OD_{600} of 1.0, harvested, and resuspended in 0.5 ml of STE10 buffer (10% [wt/wt] sucrose, 10 mM EDTA, 10 mM Tris-HCl, pH 7.5) containing a protease inhibitor cocktail (10 μM antipain, 30 μM leupeptin, 30 μM chymostatin, 1 μM pepstatin A, 1 μM PMSF, and 1 μg/ml aprotinin). Cells were then lysed by vortexing with glass beads. After lysis, 1 ml of STE10 buffer was added, and the lysate was cleared of unbroken cells by centrifugation at 500 *g*. 15 OD_{600} units (~300 μl of the lysate) were layered on top of a 20–60% linear sucrose gradient (5 ml) prepared in TE (10 mM Tris-HCl, pH 7.5, 1 mM EDTA). Samples were then centrifuged at 100,000 *g* for 18 h at 4°C using an SW50.1 rotor (Beckman Coulter) as described by Roberg et al. (1997). Fractions (~440 μl each) were collected from the top of the gradient, and the protein in each fraction was precipitated with 50% TCA and processed as described above. The data are plotted as a percent of the maximum antigenic material.

IST2 mRNA localization

Localization of *IST2* mRNA by in situ RNA hybridization using an *IST2* antisense probe labeled with digoxigenin was performed as described previously by Takizawa et al. (1997, 2000).

Online supplemental material

Videos 1–10 show time-lapse movies, at one frame per 6 s, of ER segregation tubules aligning along the mother–bud axis and entering the bud in wild-type cells (SFNY1061) expressing the ER marker Hmg1p-GFP. Videos 11–20 depict time-lapse movies at one frame per 6 s of *myo4Δ* mutant cells (SFNY1218) expressing the Hmg1p-GFP fusion protein. All supplemental material is available at http://www.jcb.org/cgi/content/full/jcb.200304030/DC1.

We thank Flora Rafi for assistance in screening the yeast deletion library, Yunrui Du for technical advice and comments on the manuscript, Yueyi Zhang for technical assistance, and Ben Glick and David Ng for providing plasmids.

This work was supported by a program project grant from the National Cancer Institute.

Submitted: 7 April 2003
Accepted: 22 October 2003

References

Antebi, A., and G.R. Fink. 1992. The yeast Ca^{2+}-ATPase homologue, PMR1, is required for normal Golgi function and localizes in a novel Golgi-like distribution. *Mol. Biol. Cell.* 3:633–654.

Barrowman, J., M. Sacher, and S. Ferro-Novick. 2000. TRAPP stably associates with the Golgi and is required for vesicle docking. *EMBO J.* 19:862–869.

Bertrand, E., P. Chartrand, M. Schaefer, S.M. Shenoy, R.H. Singer, and R.M. Long. 1998. Localization of *ASH1* mRNA particles in living yeast. *Mol. Cell.* 2:437–445.

Bevis, B.J., A.T. Hammond, C.A. Reinke, and B.S. Glick. 2002. De novo formation of transitional ER sites and Golgi structures in *Pichia pastoris*. *Nat. Cell Biol.* 4:750–756.

Bobola, N., R.P. Jansen, T.H. Shin, and K. Nasmyth. 1996. Asymmetric accumulation of Ash1p in postanaphase nuclei depends on a myosin and restricts yeast mating-type switching to mother cells. *Cell.* 84:699–709.

Boevink, P., K. Oparka, S. Santa Cruz, B. Martin, A. Betteridge, and C. Hawes. 1998. Stacks on tracks: the plant Golgi apparatus traffics on an actin/ER network. *Plant J.* 15:441–447.

Böhl, F., C. Kruse, A. Frank, D. Ferring, and R.-P. Jansen. 2000. She2p, a novel RNA-binding protein tethers ASH1 mRNA to the Myo4p myosin motor via She3p. *EMBO J.* 19:5514–5524.

Catlett, N.L., and L.S. Weisman. 1998. The terminal tail region of a yeast myosin-V mediates its attachment to vacuole membranes and sites of polarized growth. *Proc. Natl. Acad. Sci. USA.* 95:14799–14804.

Catlett, N.L., and L.S. Weisman. 2000. Divide and multiple: organelle partitioning in yeast. *Curr. Opin. Cell Biol.* 12:509–515.

Catlett, N.L., J.E. Duex, F. Tang, and L.S. Weisman. 2000. Two distinct regions in a yeast myosin-V tail domain are required for the movement of different cargoes. *J. Cell Biol.* 150:513–526.

Cheney, R.E., M.K. O'Shea, J.E. Heuser, M.V. Coelho, J.S. Wolenski, E.M. Espreafico, P. Forscher, R.E. Larson, and M.S. Mooseker. 1993. Brain myosin-V is a two-headed unconventional myosin with motor activity. *Cell.* 75: 13–23.

Du, Y., M. Pypaert, P. Novick, and S. Ferro-Novick. 2001. Aux1p/Swa2p is required for cortical endoplasmic reticulum inheritance in *Saccharomyces cerevisiae*. *Mol. Biol. Cell.* 12:2614–2628.

Fehrenbacher, K.L., D. Davis, M. Wu, I. Boldogh, and L.A. Pon. 2002. Endoplasmic reticulum dynamics, inheritance, and cytoskeletal interactions in budding yeast. *Mol. Biol. Cell.* 13:854–865.

Foissner, I., I.K. Lichtscheidl, and G.O. Wasteneys. 1996. Actin-based vesicle dynamics and exocytosis during wound wall formation in characean internodal cells. *Cell Motil. Cytoskeleton.* 35:35–48.

Franzusoff, A., K. Redding, J. Crosby, R.S. Fuller, and R. Schekman. 1991. Localization of components involved in protein transport and processing through the yeast Golgi apparatus. *J. Cell Biol.* 112:27–37.

Govindan, B., R. Bowser, and P. Novick. 1995. The role of Myo2p, a yeast class V myosin, in vesicular transport. *J. Cell Biol.* 128:1055–1068.

Hill, K., N. Catlett, and L. Weisman. 1996. Actin and myosin function in directed vacuole movement during cell division in *Saccharomyces cerevisiae*. *J. Cell Biol.* 135:1535–1549.

Holstein, S.E., H. Ungewickell, and E. Ungewickell. 1996. Mechanism of clathrin basket dissociation:separate functions of protein domains of the DnaJ homologue auxilin. *J. Cell Biol.* 135:925–937.

Itoh, T., A. Watabe, A. Toh-e, and Y. Matsui. 2002. Complex formation with Ypt11p, a rab-Type Small GTPase, is essential to facilitate the function of Myo2p, a class V myosin, in mitochondrial distribution in *Saccharomyces cerevisiae*. *Mol. Cell. Biol.* 22:7744–7757.

Jansen, R.-P., C. Dowzer, C. Michaelis, M. Galova, and K. Nasmyth. 1996. Mother cell-specific HO expression in budding yeast depends on the unconventional myosin Myo4p and other cytoplasmic proteins. *Cell.* 84:687–697.

Kachar, B., and T. Reese. 1988. The mechanism of cytoplasmic streaming in characean algal cells: sliding of endoplasmic reticulum along actin filaments. *J. Cell Biol.* 106:1545–1552.

Kruse, C., A. Jaedicke, J. Beaudouin, F. Bohl, D. Ferring, T. Guttler, J. Ellenberg, and R.-P. Jansen. 2002. Ribonucleoprotein-dependent localization of the yeast class V myosin Myo4p. *J. Cell Biol.* 159:971–982.

Long, R.M., R.H. Singer, X. Meng, I. Gonzalez, K. Nasmyth, and R.-P. Jansen. 1997. Mating type switching in yeast controlled by asymmetric localization of ASH1 mRNA. *Science.* 277:383–387.

Long, R.M., W. Gu, E. Lorimer, R.H. Singer, and P. Chartrand. 2000. She2p is a novel RNA-binding protein that recruits the Myo4p-She3p complex to ASH1 mRNA. *EMBO J.* 19:6592–6601.

Longtine, M.S., A. Mckenzie, III, D.J. Demarini, N.G. Shah, A. Wach, A. Brachat, P. Philippsen, and J.R. Pringle. 1998. Additional modules for versatile and economical PCR-based gene deletion and modification in *Saccharomyces cerevisiae*. *Yeast.* 14:953–961.

Mozdy, A.D., J.M. McCaffery, and J.M. Shaw. 2000. Dnm1p GTPase-mediated mitochondrial fission is a multi-step process requiring the novel integral membrane component Fis1p. *J. Cell Biol.* 151:367–380.

Münchow, S., C. Sauter, and R. Jansen. 1999. Association of the class V myosin Myo4p with a localised messenger RNA in budding yeast depends on She proteins. *J. Cell Sci.* 112:1511–1518.

Nakayama, K., T. Nagasu, Y. Shimma, J. Kuromitsu, and Y. Jigami. 1992. *OCH1* encodes a novel membrane-bound mannosyltransferase: outer chain elongation of asparagine-linked oligosaccharides. *EMBO J.* 11:2511–2519.

Preuss, D., J. Mulholland, C.A. Kaiser, P. Orlean, C. Albright, M.D. Rose, P.W. Robbins, and D. Botstein. 1991. Structure of the yeast endoplasmic reticulum: localization of ER proteins using immunofluorescence and immunoelectron microscopy. *Yeast.* 7:891–911.

Preuss, D., J. Mulholland, A. Franzusoff, N. Segev, and D. Botstein. 1992. Characterization of the *Saccharomyces* Golgi complex through the cell cycle by immunoelectron microscopy. *Mol. Biol. Cell.* 3:789–803.

Prinz, W.A., L. Grzyb, M. Veenhuis, J.A. Kahana, P.A. Silver, and T.A. Rapoport. 2000. Mutants affecting the structure of the cortical endoplasmic reticulum in *Saccharomyces cerevisiae*. *J. Cell Biol.* 150:461–474.

Pruyne, D.W., D.H. Schott, and A. Bretscher. 1998. Tropomyosin-containing actin cables direct the Myo2p-dependent polarized delivery of secretory vesicles in budding yeast. *J. Cell Biol.* 143:1931–1945.

Reck-Peterson, S.L., M.J. Tyska, P.J. Novick, and M.S. Mooseker. 2001. The yeast class V myosins, Myo2p and Myo4p, are nonprocessive actin-based motors. *J. Cell Biol.* 153:1121–1126.

Roberg, K.J., N. Rowley, and C.A. Kaiser. 1997. Physiological regulation of membrane protein sorting late in the secretory pathway. *J. Cell Biol.* 137: 1469–1482.

Rose, M.D., L.M. Misra, and J.P. Vogel. 1989. KAR2, a karyogamy gene, is the yeast homolog of the mammalian BiP/GRP78 gene. *Cell.* 57:1211–1221.

Rossanese, O.W., J. Soderholm, B.J. Bevis, I.B. Sears, J. O'Connor, E.K. Williamson, and B.S. Glick. 1999. Golgi structure correlates with transitional endoplasmic reticulum organization in *Pichia Pastoris* and *Saccharomyces cerevisiae*. *J. Cell Biol.* 145:69–81.

Rossanese, O.W., C.A. Reinke, B.J. Bevis, A.T. Hammond, I.B. Sears, J. O'Connor, and B.S. Glick. 2001. A role for actin, Cdc1p, and Myo2p in the inheritance of late Golgi elements in *Saccharomyces cerevisiae*. *J. Cell Biol.* 153:47–62.

Sil, A., and I. Herskowitz. 1996. Identification of asymmetrically localized determinant, Ash1p, required for lineage-specific transcription of the yeast HO gene. *Cell.* 84:711–722.

Simon, V.R., S.L. Karmon, and L.A. Pon. 1997. Mitochondrial inheritance: cell cycle and actin cable dependence of polarized mitochondrial movements in *Saccharomyces cerevisiae*. *Cell Motil. Cytoskeleton.* 37:199–210.

Tabb, J., B. Molyneaux, D. Cohen, S. Kuznetsov, and G. Langford. 1998. Transport of ER vesicles on actin filaments in neurons by myosin V. *J. Cell Sci.* 111:3221–3234.

Takizawa, P.A., and R.D. Vale. 2000. The myosin motor, Myo4p, binds Ash1 mRNA via the adapter protein, She3p. *Proc. Natl. Acad. Sci. USA.* 97: 5273–5278.

Takizawa, P.A., A. Sil, J.R. Swedlow, I. Herskowitz, and R.D. Vale. 1997. Actin-dependent localization of an RNA encoding a cell-fate determinant in yeast. *Nature.* 389:90–93.

Takizawa, P.A., J.L. DeRisi, J.E. Wilhelm, and R.D. Vale. 2000. Plasma membrane compartmentalization in yeast by messenger RNA transport and a septin diffusion barrier. *Science.* 290:341–344.

Vida, T., and S. Emr. 1995. A new vital stain for visualizing vacuolar membrane dynamics and endocytosis in yeast. *J. Cell Biol.* 128:779–792.

Wang, Y., H. Zhao, T. Harding, D. Gomes de Mesquita, C. Woldringh, D. Klionsky, A. Munn, and L. Weisman. 1996. Multiple classes of yeast mutants are defective in vacuole partitioning yet target vacuole proteins correctly. *Mol. Biol. Cell.* 7:1375–1389.

Warren, G., and W. Wickner. 1996. Organelle inheritance. *Cell.* 84:395–400.

Waterman-Storer, C.M., and E. Salmon. 1998. Endoplasmic reticulum membrane tubules are distributed by microtubules in living cells using three distinct mechanisms. *Curr. Biol.* 8:798–806.

Wilkinson, B.M., A.J. Critchley, and C.J. Stirling. 1996. Determination of the transmembrane topology of yeast Sec61p, an essential component of the endoplasmic reticulum translocation complex. *J. Biol. Chem.* 271:25590–25597.

Wöllert, T., D.G. Weiss, H.H. Gerdes, and S.A. Kuznetsov. 2002. Activation of myosin V-based motility and F-actin-dependent network formation of endoplasmic reticulum during mitosis. *J. Cell Biol.* 159:571–577.

Wu, X., B. Bowers, Q. Wei, B. Kocher, and J. Hammer. 1997. Myosin V associates with melanosomes in mouse melanocytes: evidence that myosin V is an organelle motor. *J. Cell Sci.* 110:847–859.

Yaffe, M.P. 1999. The machinery of mitochondrial inheritance and behavior. *Science.* 283:1493–1497.

Yin, H., D. Pruyne, T.C. Huffaker, and A. Bretscher. 2000. Myosin V orientates the mitotic spindle in yeast. *Nature.* 406:1013–1015.